HYDROTHERMAL TRANSFORMATION OF KAOLINITE IN THE SYSTEM K_2O-SiO_2-Al_2O_3-H_2O

TRANSFORMACIÓN HIDROTERMICA DE CAOLINITA EN EL SISTEMA K_2O-SiO_2-Al_2O_3-H_2O

CARLOS ALBERTO RIOS REYES
Universidad Industrial de Santander, Bucaramanga, Colombia, carios@uis.edu.co

CRAIG DENVER WILLIAMS
University of Wolverhampton, Wulfruna Street, Wolverhampton WV1 1SB, England, c.williams@wlv.ac.uk

Received for review July 24 th, 2009, accepted March 3 th, 2010, final version March, 18 th, 2010

ABSTRACT: A kaolinite-rich raw material was treated hydrothermally with 1.33 and 3.99M KOH solutions at 100 and 175 °C during different reaction times ranging from 24 to 528 h. The synthesis products were characterized by X-ray diffraction, scanning electron microscopy, Fourier transform infrared spectroscopy, magic angle spinning nuclear magnetic resonance and thermogravimetric analysis in order to elucidate their physicochemical and mineralogical characteristics. The transformation of the starting material in KOH solutions can be explained by two different processes: (1) dissolution and (2) precipitation. A series of crystalline phases summarized by the reaction sequence kaolinite → chabazite → edingtonite → unidentified potassium aluminosilicate phase → kalsilite + leucite was identified in the system K_2O-SiO_2-Al_2O_3-H_2O. The solid products show, on the other hand, remarkable textural and structural differences with the starting material.

KEYWORDS: Kaolinite, potassium hydroxide, zeolites, dissolution, precipitation

RESUMEN: Una materia prima rica en caolinita fue tratada hidrotérmicamente con soluciones de KOH 1.33 y 3.99M a 100 y 175 °C durante diferentes tiempos de reacción variando de 24 a 528 h. Los productos sintéticos fueron caracterizados por difracción de rayos X, microscopia electrónica de barrido, espectroscopia infrarrojo por transformada de Fourier, resonancia magnética nuclear con rotación en ángulo mágico y análisis termogravimétrico con el fin de establecer sus características fisicoquímicas y mineralógicas. La transformación del material de partida en soluciones de KOH pueden explicarse a partir de dos procesos diferentes: (1) disolución y (2) precipitación. Una serie de fases cristalinas resumidas por la secuencia de reacción caolinita → chabazita → edingtonita → fase de aluminosilicato potásico no identificada → kalsilita + leucita fue identificada en el sistema K_2O-SiO_2-Al_2O_3-H_2O. Los productos sólidos, muestran, por otra parte, notables diferencias texturales y estructurales con el material de partida.

PALABRAS CLAVE: Caolinita, hidróxido de potasio, zeolitas, disolución, precipitación

1. INTRODUCTION

Kaolinite is not stable under highly alkaline conditions and different zeolitic materials can form. According to Zhao *et al.* [1], there are two major chemical processes involved in the reaction between kaolinite and alkaline solutions: dissolution of kaolinite, releasing Si and Al, followed formation of zeolitic materials. The kaolinite-rich raw material used in this study has been used by Ríos and co-workers [2-5] as the Al and Si sources for the synthesis of several types of zeolites in alkaline media. Experimental data from the syntheses in potassium aluminosilicate systems are contradictory and confusing [4]. In addition, the nomenclature for potassium zeolites has evolved over a period of decades since the early

discovery of hydrothermal synthesis routes by Barrer [6]. A crystallization sequence illite → zeolite K-F → K-phillipsite → K-feldspar, reported by Bauer *et al.* [7] was monitored during the hydrothermal treatment of kaolinite-rich raw material in KOH solutions. In this work, we investigate the hydrothermal transformation of kaolinite into zeolites by the conventional hydrothermal synthesis. However, a different reaction sequence was documented, due to the probable absence of illite and the presence of three metastable phases (chabazite, edingtonite and unidentified potassium aluminosilicate) and two stable final crystalline phases (kalsilite and leucite). On the other hand, activation of kaolinite was carried out at shorter reaction times compared with those used by Bauer *et al.* [7].

2. EXPERIMENTAL

2.1 Materials

Kaolinite (≤ 2 μm), $Al_2SiO_5(OH)_4$, was used as starting material for zeolite synthesis. It is distributed under the name Supreme Powder supplied by ECC International. Other reagents used in the activation of kaolinite were: potassium hydroxide, KOH, as pellets (> 85%, Aldrich Chemical Company, Inc.) and distilled water using standard purification methods.

2.2 Synthesis of zeolite-types

The conversion of kaolinite into zeolitic materials was conducted by the conventional hydrothermal synthesis as follows: in reaction plastic beakers (150-250 ml), a calculated amount of KOH in pellets (1.35 or 4.03 g) was added to distilled water (18 ml) to prepare KOH solutions 1.33 or 3.99M, and then 3.10 g of kaolinite was added to the alkaline solutions. The progressive addition of reagents was carried out under stirring conditions until they dissolved to homogenize the reaction gels. Crystallization was carried out by hydrothermal synthesis under static conditions in PTFE vessels of 65 ml at 100°C and in teflon lined stainless steel autoclaves of 20 ml at 175°C for several reaction times. Table 1 summarizes the starting reaction conditions for the conversion of kaolinite into zeolites in KOH solutions. Once the activation time was reached, the reactors were removed from the oven and quenched in cold water to stop the reaction. After hydrothermal treatment, the reaction mixtures were filtered and washed with distilled water to remove excess alkali until the pH of the filtrate became neutral. Then, the samples were oven dried at 80°C overnight. Ph of the reaction gels was measured before and after hydrothermal treatment. The dried samples were weighed and kept in plastic bags for characterization.

Table 1. Experimental conditions of kaolinite activation into zeolitic materials

Test	Chemical reagents			L/S	Hydrothermal reaction		Molar gel composition	Zeolitic phases and other synthesis products
	H_2O (g)	KOH (g)	KAO (g)	(ml/g)	T / °c	t / h		
1	18,00	1,35	3,10	6,24	100	27	$K_2O:Al_2O_3:2SiO_2:86.3H_2O$	CHA
2	18,00	1,35	3,10	6,24	100	240	$K_2O:Al_2O_3:2SiO_2:86.3H_2O$	CHA
3	18,00	1,35	3,10	6,24	100	528	$K_2O:Al_2O_3:2SiO_2:86.3H_2O$	CHA
4	18,00	4,03	3,10	7,11	100	27	$3K_2O:Al_2O_3:2SiO_2:88.3H_2O$	CHA, EDI
5	18,00	4,03	3,10	7,11	100	240	$3K_2O:Al_2O_3:2SiO_2:88.3H_2O$	CHA, EDI
6	18,00	4,03	3,10	7,11	100	528	$3K_2O:Al_2O_3:2SiO_2:88.3H_2O$	CHA, EDI
7	18,00	1,35	3,10	6,24	175	24	$K_2O:Al_2O_3:2SiO_2:86.3H_2O$	EDI
8	18,00	1,35	3,10	6,24	175	216	$K_2O:Al_2O_3:2SiO_2:86.3H_2O$	EDI
9	18,00	1,35	3,10	6,24	175	312	$K_2O:Al_2O_3:2SiO_2:86.3H_2O$	EDI
10	18,00	4,03	3,10	7,11	175	24	$3K_2O:Al_2O_3:2SiO_2:88.3H_2O$	Kal, Leu
11	18,00	4,03	3,10	7,11	175	216	$3K_2O:Al_2O_3:2SiO_2:88.3H_2O$	Kal, Leu
12	18,00	4,03	3,10	7,11	175	312	$3K_2O:Al_2O_3:2SiO_2:88.3H_2O$	Kal, Leu

CHA, chabazite; EDI, zeolite Barrer-KF; Kal, kalsilite; Leu, leucite; KAO, kaolinite; L/S, activator solution/KAO ratio.

2.3 Characterization

X-ray diffraction patterns of the untreated kaolinite and synthesis products were recorded using a Philips PW1710 diffractometer operating in Bragg-Brentano geometry with Cu-Kα radiation (40 kV and 40 mA) and secondary monochromation. Data collection was carried out in the 2θ range 3-50°, with a step size of 0.02°. Phase identification was performed by searching the ICDD powder diffraction file database, with the help of JCPDS (Joint Committee on Powder Diffraction Standards) files for inorganic compounds. The relative intensity yields were obtained from normalized XRD intensities of the major reflection for each material. The morphology of the solid phases were examined by scanning electron microscopy (ZEISS EVO50) and the chemical composition of mineral phases was studied using the EDXS mode, under the following analytical conditions:

I probe 1 nA, EHT = 20.00 kV, beam current 100 µA, Signal A = SE1, WD = 8.0 mm. Fourier transform infrared (FTIR) spectroscopy was carried out using a Mattson Genesis II FTIR spectrometer in the 4000-400 cm^{-1} region. However, we discuss only the 1200-400 cm^{-1} region, because there spectra showed remarkable changes. Magic Angle Spinning Nuclear Magnetic Resonance (MAS NMR) spectra for ^{29}Si and ^{27}Al, respectively, were recorded at room temperature on a Varian Unity INOVA spectrometer under the following analytical conditions: MAS probe 7.5 and 4.0 mm; frequency 59.6 and 78.1 MHz; spectral width 29996.3 and 100000.0 Hz; acquisition time 30 and 10 µs; recycle time 120 and 0.5 s; number of repetitions 15 and 2200; spinning rate 5040 and 14000 Hz; pulse angle (DP) 90.0 and 18.9°. The chemical shifts were referenced to tetramethylsilane (TMS) for ^{29}Si and 1 M $AlCl_3$ aqueous solution for ^{27}Al. Thermogravimetry was performed on a Mettler Toledo TG50 thermobalance in the temperature range of 25–700 °C, with a heating rate of 10 °C min^{-1} under flowing air. Mass losses were determined by employing both TGA and DTG curves. The second derivative differential thermal curve was used for peak temperature determinations.

3. RESULTS AND DISCUSSIONS

3.1 Chemical and mineralogical analyses of the starting material

As shown in the XRD pattern (Figure 1), kaolinite is the predominant mineral phase, which can be identified by its characteristic XRD peaks at 12.34° and 24.64° 2θ as reported by Zhao *et al.* [1]. However, minor impurities, such as illite, muscovite and halloysite, also occur. Kaolinite can be recognized by its platy morphology and hexagonal outlines (Figure 1), with small well-formed hexagonal plates loosely packed, defining an orientation.

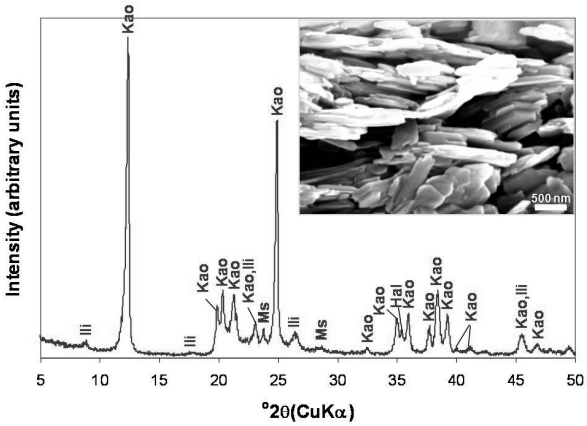

Figure 1. X-ray diffraction pattern and SEM image of the starting material. Kao, Kaolinite; Ili, illite; Ms, muscovite; Hal, halloysite

3.2 Zeolite characterization

3.2.1 X-ray diffraction analysis

The XRD patterns in Figure 2 reveals that the hydrothermal treatment of kaolinite in KOH solutions is characterized by the dissolution of the starting material and the formation of amorphous and crystalline aluminosilicate phases (three metastable phases, chabazite, edingtonite and an unidentified potassium aluminosilicate, and two stable phases, kalsilite and leucite). The unidentified peaks in the XRD patterns should represent the still remaining kaolinite or some potassium aluminosilicate phases.

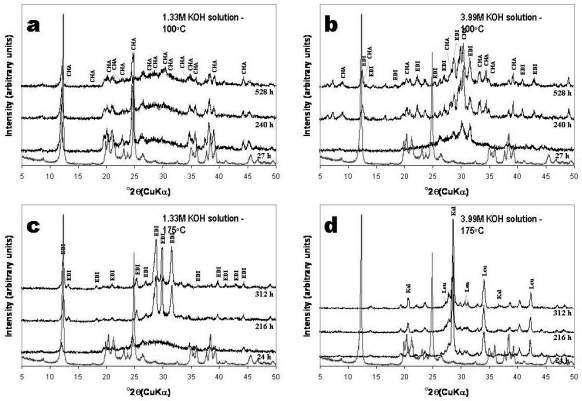

Figure 2. X-ray diffraction patterns of the starting material (in red) and representative as-synthesized products obtained after hydrothermal reaction of the starting material in KOH solutions. KAO, kaolinite; CHA, chabazite; EDI, edingtonite; Kal, kalsilite; Leu, leuc

As can be seen from the XRD patterns in Figure 2a, very weak peaks indicate that chabazite was the only crystalline phase formed when a low KOH concentration and temperature were used. There was no change in peak intensity over 240-528 h period. At high KOH concentration (Figure 2b), an intense dissolution of the raw material was accompanied by the precipitation of three different zeolitic phases (chabazite and edingtonite, which increased with reaction time. However, it could be said that KOH concentration increase promoted the edingtonite formation. Figure 2c shows that this zeolite crystallized at low KOH concentration and high temperature, although its peak intensity tended to be constant over 216-312 h period, with a large amount of amorphous aluminosilicate material at shorter reaction times (24 h), as evident by a hump between 25 and 35^{o} 2θ. The increase in temperature had a negative effect in chabazite formation. The XRD patterns in Figure 2d show that a mixture of kalsilite ($KAlSiO_4$) and leucite ($KAlSi_2O_6$) formed at high KOH concentration and temperature, without a change in peak intensity during the monitoring time.

3.2.2 Scanning electron microscopy

SEM images (Figures 3 and 4) shows interesting morphologies that provide new evidence on the phase reaction history after the hydrothermal transformation of kaolinite in KOH solutions.

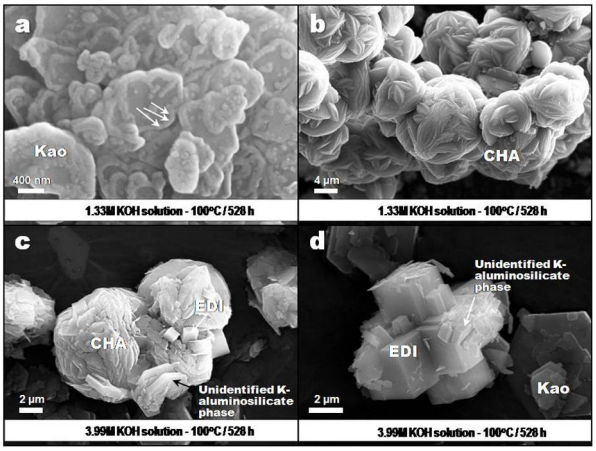

Figure 3. SEM images showing the occurrence of representative synthesis products obtained via hydrothermal treatment of kaolinite in KOH solutions at 100 ^{o}C. Kao, kaolinita; CHA, chabazite; EDI, edingtonite

Figure 3a illustrates an example of the dissolution of kaolinite, revealed by its different morphology in the boundary region, which may indicate the formation of illite. The arrows indicate the position of developed illite. However, the Initial precipitation of the metastable chabazite could affect the activity of K and inhibits precipitation of illite. On the other hand, some Fe should be released by dissolution of impurities in kaolinite to promote the formation of illite. Figure 3b illustrates aggregates of cauliflower-shape morphology of bladed crystals of chabazite.In Figure 3c is revealed the presence of neoformed crystals of edingtonite and an unidentified potassium aluminosilicate, which have grown at the expense of spheroidal aggregates of chabazite. An intergrowth between prismatic crystals of edingtonite developing cruciform penetrating twinning and a potassium aluminosilicate phase with hexagonal plate-like morphology is illustrated in Figure 3d. Observe also the occurrence of stacks of face-to-face relict kaolinite flakes with euhedral pseudohexagonal crystals with regular edges. The hexagonal morphology of the unidentified potassium aluminosilicate is similar to that observed in the hexagonal polymorph of faujasite (EMT) or in the zeolite MCM-61 (MSO), which have been synthesized only in the presence of 1,4,7,10,13,16-hexaoxacyclooctadecane (18-Crown-6) [8-10] or using 18-Crown-6 in the presence of potassium cations [11], respectively. In spite of XRD and SEM data providing some evidences on the presence of a potassium aluminosilicate phase associated to chabazite and edingtonite, it is difficult to speculate that this phase could correspond to the EMT or MSO-type structure.

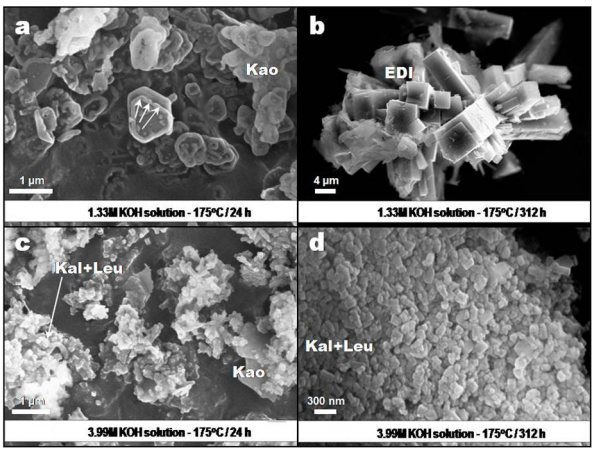

Figure 4. SEM images showing the occurrence of representative synthesis products obtained via hydrothermal treatment of kaolinite in KOH solutions at 175 ^{o}C. Kao, kaolinita; Kal, kalsilite; Leu, leucite

Figure 4a shows an additional evidence of the dissolution of kaolinite (as indicated by the arrows) at low KOH concentration and reaction time and high temperature, comparable with what is observed in Figure 3a. In Figure 4b is illustrated a radial array of tetragonal prismatic crystals of edingtonite, which grew from the centre of a spherule, showing a typical growth mechanism from a nucleating point in an essentially amorphous material. A similar morphology for edingtonite has been achieved by Juan *et al.* [12] after activation of fly ash in KOH solutions at 150 ^{o}C. As shown in Figure 4c, flaky and blocky morphologies reveal the presence of the starting material along with a very fine grain-sized aggregate of kalsilite and leucite. The occurrence of these potassium aluminosilicates is illustrated in Figure 4d. It is proposed that after kaolinite dissolution in KOH solutions, chabazite represents the first zeolitic phase that crystallized, followed by a crystallization of edingtonite, which is progressively accompanied by the presence of an additional potassium aluminosilicate phase, developing intergrowths with edingtonite, and finally the formation of the stable mixture composed by kalsilite and leucite.

Under experimental conditions similar to those used in this study, Barrer [6] demonstrated the formation of zeolite K-F (edingtonite-type structure) predominantly at temperatures between 80-170 ^{o}C over a range of KOH concentrations. Chabazite stability is controlled by KOH concentration and temperature, whereas edingtonite formation is promoted increasing KOH molarity and temperature. According to Mackinnon *et al.* [13], at high temperatures (200-350 ^{o}C), the dominant potassium aluminosilicate phase is either kalsilite or kaliophyllite depending on the starting composition. Syntheses at higher temperatures favour the crystallization of leucite and analcime [14]. However, the synthesis of stable phases, such as kalsilite and leucite, at lower temperature (175 ^{o}C) have been demonstrated in this study, different to what is reported by these authors.

3.2.3 Fourier transform infrared spectroscopy

Figure 5 illustrates the FTIR spectra of the raw material and as-synthesized products obtained after its hydrothermal treatment in KOH solutions. The characteristic peaks of the kaolinite spectrum weakened, just showing a small decrease with reaction time, although did not disappear after activation of kaolinite in 1.33M KOH solutions at 100 ^{o}C (1 and 3 spectra). On the other hand, when the reaction was carried out in 3.99M KOH solutions at 100 ^{o}C (4 and 6 spectra), they disappeared accompanied by the appearance of new vibration bands as follows. In the region of 1200-850 cm^{-1}, a peak centred at 976 cm^{-1} (spectrum 4) moved to a lower frequency (953 cm^{-1}, spectrum 6) with reaction time. An additional peak at 862 cm^{-1} was seen at shorter reaction time. In the region of 850-550 cm^{-1}, two different peaks appeared, 704 and 677 cm^{-1}(spectrum 4), which shifted to higher (729 cm^{-1}) and lower (662 cm^{-1}) frequencies, respectively, with reaction time, accompanied by an additional peak at 594 cm^{-1} (spectrum 6). In the region of 550-400 cm^{-1}, the vibration bands tended to disappear.

At 175 ^{o}C and low KOH concentration, peaks centred at 1007 and 874 cm^{-1} (spectrum 7) disappeared and new very weak peaks appeared with reaction time (spectrum 9). At 175 ^{o}C and high KOH concentration, the synthesis products are characterized by much better absortion bands (10 and 12 spectra), with sharp peaks revealing a material of high grade of crystallinity, which has

a very constant behaviour during the monitoring time. Several vibration bands particularly in the 850-550 cm^{-1} (T-O-T symmetrical stretching mode) and 550-400 cm^{-1} (T-O bending mode). The vibrations bands at 474, 564, 606, 682 and 964 cm^{-1} and at 461, 564 and 606 cm^{-1} can be assigned to the presence of kalsilite and leucite, respectively. These assignments correspond to the spectra reported by Dimitrijevic and Dondur [15].

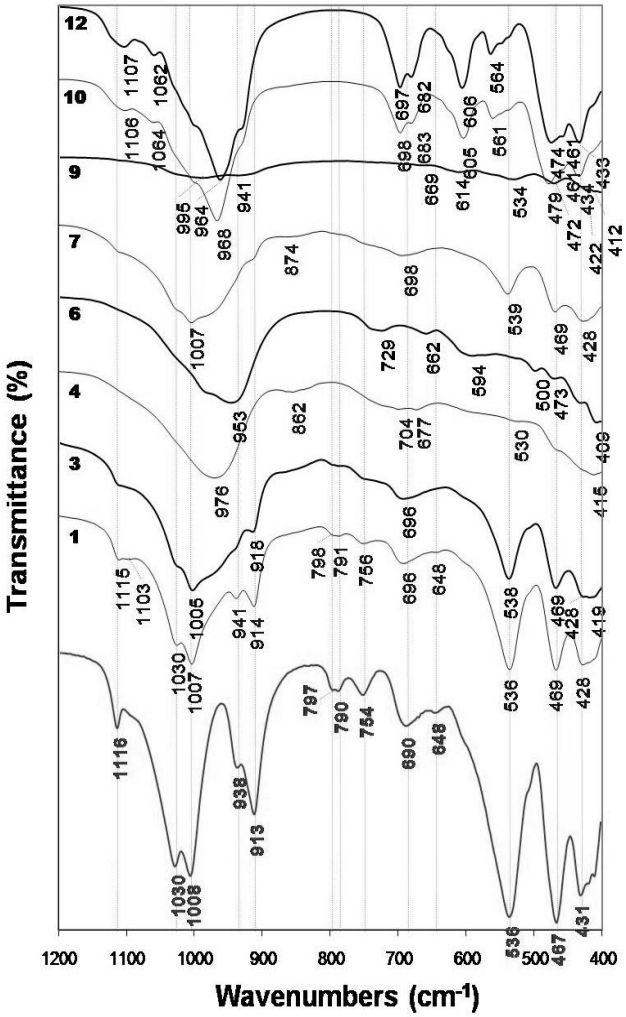

Figure 5. FTIR spectra of the unreacted (in red) kaolinite and representative as-synthesized products obtained after hydrothermal reaction of kaolinite in KOH solutions

3.2.4 ^{29}Si and ^{27}Al magic angle spinning nuclear magnetic resonance

Figure 6 shows the ^{29}Si and ^{27}Al MAS NMR spectra of the starting material and representative synthesis products obtained using KOH as an activator agent. Many important properties of zeolites are strongly dependent of the location of Si and Al in the tetrahedral framework and ^{29}Si and ^{27}Al NMR have a great potential in the direct determination of local Si and Al orderings [16].

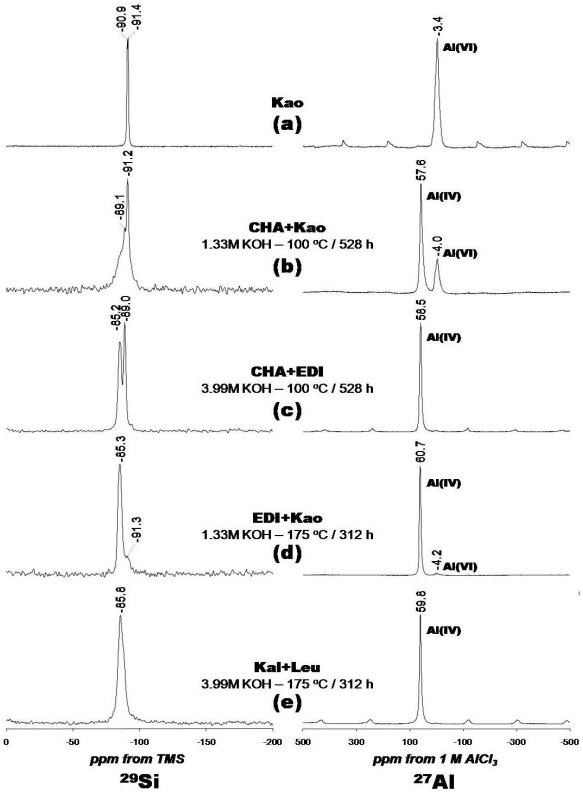

Figure 6. ^{29}Si and ^{27}Al NMR spectra of the (a) kaolinite and (b-e) representative synthesis products obtained by alkaline activation of kaolinite with KOH solutions. Kao, kaolinite; CHA, chabazite; EDI, edingtonite; Kal, kalsilite; Leu, leucite

The ^{29}Si MAS NMR spectrum of kaolinite is given on Figure 6a shows two signals at -90.9 and -91.4 ppm corresponding to different but equally populated silicon sites in kaolinite. Figure 6b shows a spectrum with a sharp peak centred at -91.2 ppm attributed to residual kaolinite that is superimposed on a broader resonance at -89.1 ppm, which can be presumably attributed to $Q^4(4Al)$ sites of chabazite and is characteristic of amorphous or poorly crystallized materials. Two well resolved resonances at -85.2 and -89.0 ppm are distinguished in Figure 6c, indicating the presence of edingtonite and chabazite, respectively. These peaks can be attributed to

Q^4(4Al) sites in the zeolite phases. Figure 6d shows a resonance at -85.3 ppm that can be attributed to Q^4(4Al) sites in edingtonite (Si/Al ratio = 1.0). A weak signal - 91.3 ppm, revealing the presence of Q^4(4Al) sites, corresponding with the presence of unreacted kaolinite. A single resonance at -85.8 ppm (Figure 6e) can be attributed to the presence of Q^4(4Al) sites of kalsilite and leucite. Barbosa and MacKenzie [17] have reported a similar signal for these potassium aluminosilicates in geopolymers. The ^{27}Al MAS NMR spectrum of the unreacted kaolinite (Figure 6a) consists of a single resonance at -3.4 ppm and is largely octahedral aluminium. Strong resonances at 57.6, 58.5, 60.7 and 59.8 ppm, respectively, can be assigned to tetrahedral Al in the framework of the zeolitic products (Figures 6b, 6c, 6d and 6e). However, in Figures 6b and 6d, weak signals at -4.0 and -4.2 ppm, respectively, correspond to residual kaolinite as revealed by the small amount of Al in octahedral sites. The amount of Al(6) was greatest in kaolinite (Figure 6a) where the initial Al concentration was larger compared with that in the synthesis products (Figures 6b-6e). ^{29}Si and ^{27}Al MAS NMR results indicates that kaolinite was or total or partially dissolved (as revealed by the signals corresponding to residual kaolinite in some of the synthesis products), in agreement with XRD and FTIR results.

3.2.5 Thermogravimetric analysis

Figure 7 shows TG/DTG curves obtained for representative as-synthesized products obtained after hydrothermal reaction of kaolinite in KOH solutions. The as-synthesized zeolitic materials show up to four dehydration steps, which could be explained as a consequence of water molecules dehydrated at lower temperatures that could re-enter the zeolite with or without affecting its framework linkages. The position of these DTG peaks and the number of dehydration steps has been attributed to the different compensating cation-water binding energies, as well as to the different energy associated with the diffusion of the desorbed water through the porous structure of the zeolitic materials [18]. The first group of peaks are in the range of 25-90 °C and correspond to water desorption; the second group of peaks are in the range of 150-300 °C and are attributed to occluded water. The occurrence of a peak at 490 °C (Figure 7a) can be attributed to framework dehydroxylation of kaolinite still remaining in the synthesis product obtained after hydrothermal reaction of kaolinte in low concentration KOH solutions, which is not observed in Figure 7b. This can be explained due to the complete reaction of the starting kaolinite in high concentration KOH solutions.

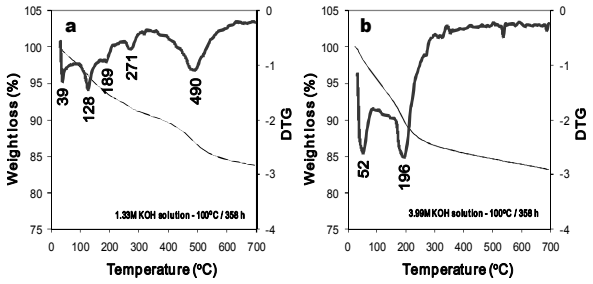

Figure 7. TG/DTG curves in the temperature range 25-700 °C of representative synthesis products obtained after alkaline activation of kaolinite using KOH as activator agent

4. CONCLUSIONS

Several zeolite-types were successfully synthesized from kaolinite by hydrothermal treatment under the selected experimental conditions in the system K_2O-SiO_2-Al_2O_3-H_2O. The synthesis products synthesized were chabazite and edingtonite, which can be accompanied by unidentified potassium aluminosilicate phases and feldspathoids (kalsilite and leucite). In general, the synthesis products are characterized by the occurrence of a large amount of an amorphous aluminosilicate phase from which several crystalline phases formed. A total dissolution of kaolinite was achieved with high KOH concentration and temperature, with an amorphous potassium aluminosilicate phase at shorter reaction times. Longer reaction times were required to obtain crystalline phases (zeolites). Therefore, to achieve a similar level of attack on kaolinite with KOH compared to that using NaOH, it would be necessary to use higher KOH concentrations, alkaline solution/KAO ratios and longer reaction times, under controlled experimental conditions, to obtain the desired zeolitic phases.

ACKNOWLEDGMENTS

We gratefully acknowledge the Programme Alban, the European Union Programme of High Level Scholarships for Latin America, scholarship No. E05D060429CO, and the Universidad Industrial de Santander (a remunerated commission) for funding C.A. Ríos. Special thanks to School of Applied Sciences at University of Wolverhampton for allowing us the use of the research facilities. We thank to Dr David Townrow and Mrs Barbara Hodson for assistance in collecting XRD and SEM data, respectively, and to Dr David Apperley and the EPSRC solid state NMR Service, University of Durham, for MAS NMR spectra.

REFERENCES

[1] ZHAO, H., DENG, Y., HARSH, J. B., FLURY, M. AND BOYLE, J. S. Alteration of Kaolinite to Cancrinite and Sodalite by Simulated Hanford Tank Waste and its impact on Cesium retention. Clays Clay Miner. 52, 1-13, 2004.

[2] RÍOS, C. A., WILLIAMS, C. D. AND CASTELLANOS, O. M. Synthesis and characterization of zeolites by activation of kaolinite and industrial by-products (fly ash and natural clinker) in alkaline solutions, Bistua 4, 60-71, 2006.

[3] RÍOS C. A., WILLIAMS, C. D. AND MAPLE, M. J. Synthesis of zeolites and zeotypes by hydrothermal transformation of kaolinite and metakaolinite, Bistua 5, 15-26, 2007.

[4] RÍOS, C. A. Synthesis of zeolites from geological materials and industrial wastes for potential application in environmental problems [PhD Thesis]. Wolverhampton, West Midlands: University of Wolverhampton, 2008.

[5] RÍOS, C. A., WILLIAMS, C. D. AND FULLEN, M. A. Nucleation and growth history of zeolite LTA synthesized from kaolinite by two different methods, Appl. Clay Sci. 42, 446–454, 2009.

[6] BARRER, R. M. Zeolites and Clay Minerals as Sorbents and Molecular Sieves. Academic Press, London, 1978.

[7] BAUER, A., VELDE, B. AND BERGER, G. Kaolinite transformation in high molar KOH solutions, Appl. Geochem. 13, 619-629, 1998.

[8] ANNEN, M. J., YOUNG, D., ARHANCET, J. P., DAVIS, M. E. AND SCHRAMM, S. Investigations into the nature of the hexagonal polytype of faujasite, Zeolites 11, 98-102, 1991.

[9] DOUGNIER, F., PATARIN, J., GUTH, J. L. AND ANGLEROT, D. Synthesis, characterization, and catalytic properties of silica-rich faujasite-type zeolite (FAU) and its hexagonal analog (EMT) prepared by using crown-ethers as templates, Zeolites 12, 160-166, 1992.

[10] BURKETT, S. L. AND DAVIS, M. E. Structure-directing effects in the crown ether-mediated syntheses of FAU and EMT zeolites, Micropor. Mater. 1, 265-282, 1993.

[11] SHANTZ, D. F., BURTON, A. AND LOBO, R. F. Synthesis, structure solution, and characterization of the aluminosilicate MCM-61: the first aluminosilicate clathrate with 18-membered rings, Micropor. Mesopor. Mater. 31, 61-73, 1999.

[12] JUAN, R., HERNÁNDEZ, S., ANDRÉS, J. M. AND RUIZ, C. Synthesis of granular zeolitic materials with high cation exchange capacity from agglomerated fly ash, Fuel 86, 1811-1821, 2007.

[13] MACKINNON, I., MILLAR, G. AND STOLZ, W. U.S. Patent No. 0 269 472, 2006.

[14] BARRER, R. M. AND MARCILLY, C. Hydrothermal chemistry of silicates. Part XV. Synthesis and nature of some salt-bearing aluminosilicates, J. Chem. Soc. (A), 2735-2745, 1970.

[15] DIMITRIJEVIC, R. AND DONDUR, V. Synthesis and characterization of $KAlSiO_4$ polymorphs on the SiO_2-$KAlO_2$ join, J. Solid State Chem. 115, 214-224, 1995.

[16] MEFTAH, M., OUESLATI, W. AND BEN HAJ AMARA, A. Synthesis process of zeolite P using a poorly crystallized kaolinite, Physics Procedia 2, 1081-1086, 2009.

[17] BARBOSA, V. F. F. AND MACKENZIE, K. J. D. Synthesis and thermal behaviour of potassium sialate geopolymers, Materials Lett. 57, 1477-1482, 2003.

[18] COVARRUBIAS, C., GARCIA, R., ARRIAGADA, R., YANEZ, J. AND GARLAND, T. Cr(III) exchange on zeolites obtained from kaolin and natural mordenite, Micropor. Mesopor. Mater. 88, 220-231, 2006.